TMI-2 Core Bore Examination Results[a]

C. S. Olsen, D. W. Akers, and R. K. McCardell
Idaho National Engineering Laboratory
EG&G Idaho Inc.
Idaho Falls, Idaho 83415

ABSTRACT

Examinations are being performed on samples obtained from the lower portion of the TMI-2 reactor core as part of the TMI-2 Sample Acquisition and Examination Program. This paper presents preliminary results of visual examinations, the gamma spectrometry analyses performed on the intact core bores, and the metallurgical examinations. These examinations indicate significant core damage effects on the distribution of core materials and fission products in the lower reactor core including the substantial relocation and segregation of some fission products (e.g., Sb-125 and Ru-106).

INTRODUCTION

Unit 2 of the Three Mile Island pressurized water reactor underwent a loss-of-coolant accident on March 28, 1979, resulting in severe damage to the reactor core. After the accident, four organizations, General Public Utilities Nuclear Corporation (GPU Nuclear), the Electric Power Research Institute (EPRI), the Nuclear Regulatory Commission (NRC), and the Department of Energy (DOE), collectively known as GEND, cosponsored a postaccident evaluation of the TMI-2 accident. During 1986, a core boring operation was conducted jointly by EG&G Idaho, Inc. and GPU Nuclear to obtain samples of the lower reactor core necessary to spatially characterize the chemical and physical state of this part of the degraded core.[1]. The results of these examinations will be used to provide data on fission product release, interaction between core components, hydrogen generation, and core melt progression.

Previous examinations of the reactor core indicated that the upper reactor core contained a void region almost entirely surrounded by standing peripheral assemblies (Figure 1). Below the void region was a layer of loose debris resting on a hard crust[2]. However, conditions in the region of the core below the debris bed (approximately 50 percent of the core volume) were not known as there were no penetrations through the crust layer. Consequently, to examine this portion of the reactor core, a core boring system capable of penetrating the hard crust was developed to provide access to the lower core region for both examination and defueling purposes. The

a. Work supported by the U.S. Department of Energy, Assistant Secretary for Nuclear Energy, Office of Light Water Reactor Safety and Technology, under DOE contract Number DE-AC07-76-ID01570.

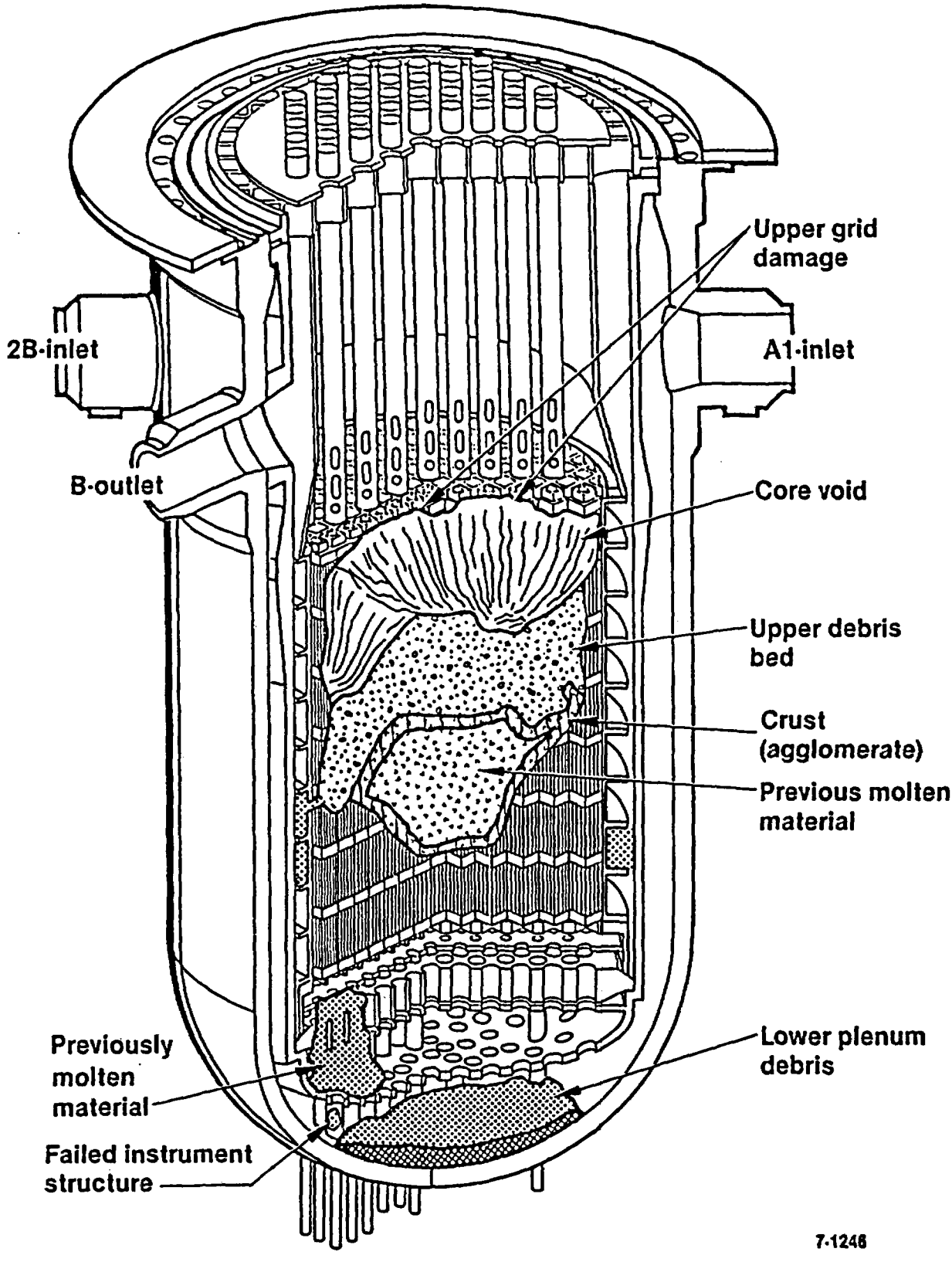

Figure 1. End state condition of the TMI-2 reactor core.

core boring operations were performed during July and August 1986 and the bores acquired were transported to the Idaho National Engineering Laboratory(INEL) for sectioning and distribution of the samples to laboratories participating in the core bore examinations. The initial results of the examinations performed at the INEL are the subject of this paper.

The core bores extracted from the lower core region were obtained from nine pre-selected locations. These core locations were chosen to spatially characterize the current chemical and physical state of the reactor core and to define the distribution of core structural materials within the lower reactor vessel. The samples produced from the coring operation in the reactor vessel were discontinuous bores of fuel material which were approximately 2 m long and 6.4 cm in diameter. Only small amounts of material (i.e., a few grams) were obtained from the lower reactor vessel head cores due to the small particle size of much of the debris located there.

Following the delivery of the cores to the INEL, a series of physical, metallurgical, and radiochemical measurements were begun on specimens from the core bores. The physical measurements which were performed to characterize the general physical characteristics of the debris, include dry weight, immersion density, open porosity, and radiation levels. Metallurgical examinations were performed to characterize the full range of metallurgical properties of the debris (e. g., grain size, composition, oxygen content, etc.) using optical metallography and scanning electron microscopy with energy dispersive x-ray (EDX) analysis and wavelength dispersive x-ray (WDX) analysis. The radiochemical measurements are being performed to determine the chemical composition of the debris and to define the extent of radionuclide retention in the debris. Measurement techniques being used include gamma spectroscopy, neutron activation analysis, liquid scintillation analysis, and mass spectrometry. Results included in this paper are from the visual examinations, the gamma spectrometry analyses performed on the intact core bores and some of the metallurgical analyses. (Not all examinations were complete at the time this paper was prepared.)

VISUAL APPEARANCE AND DENSITY MEASUREMENTS

During the core boring operation, video inspections of the interior of each core bore hole were performed to characterize the lower core and the region immediately below the bottom of the core (the core support assembly region)[3]. These videos indicated that the core below the upper debris bed consisted of two regions: (a) a region of previously molten core materials surrounded by a hard crust, and (b) a region of intact standing fuel rods extending from the bottom of the previously molten region to the bottom of the core.

When the core bores were removed from their split tubes, visual examinations indicated that they contained solid plugs of the upper and lower crusts, previously molten material from between the crusts, and fuel rod stubs (Figure 2). The solid plugs from the upper and lower crusts were generally composed of agglomerated fuel and structural material components.

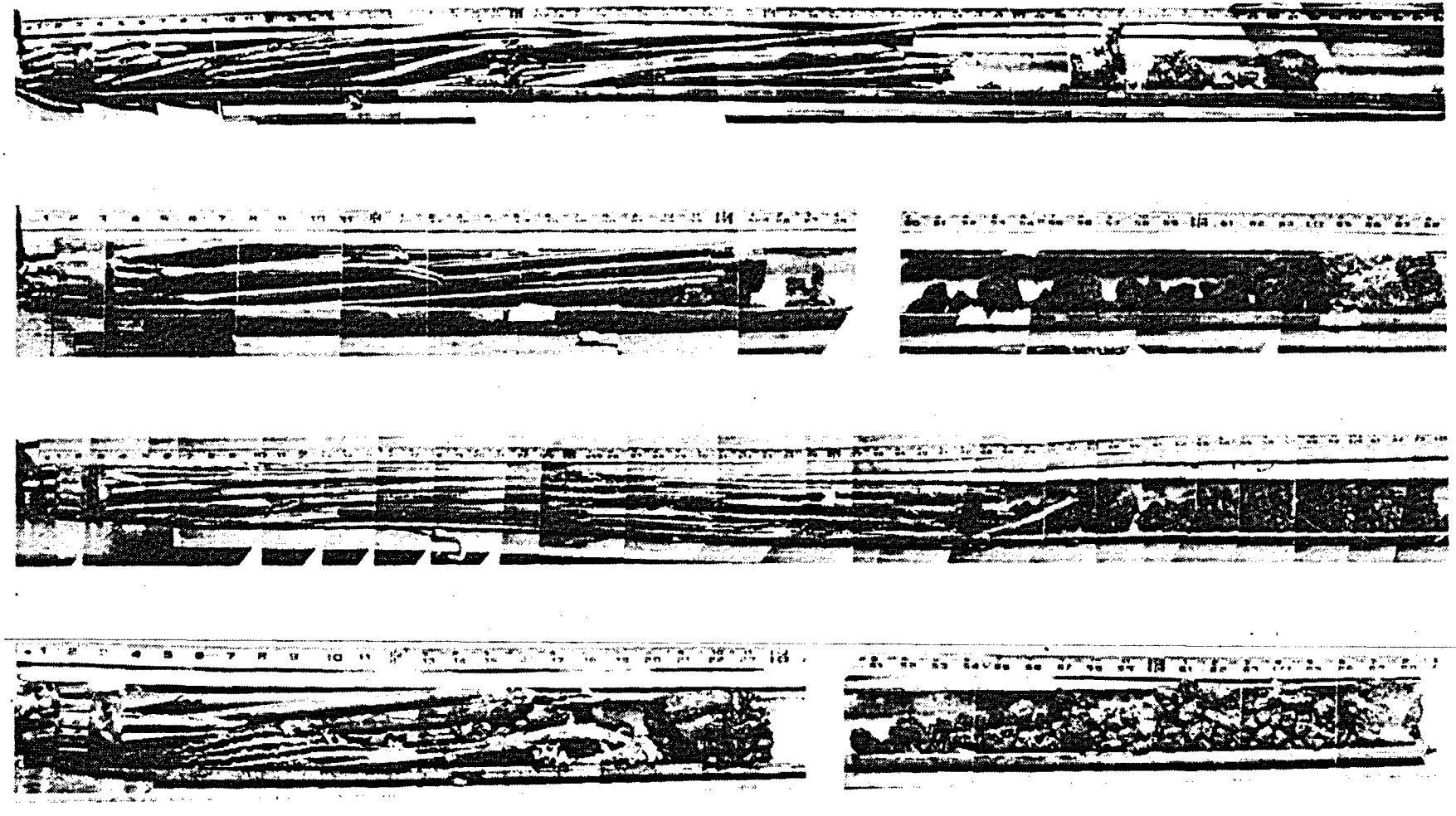

Figure 2. Principle core bore samples--core locations D8, G8, G12, and G9 from the top.

The upper crust samples were composed of a mixture of debris agglomerated with substantial amounts of metallic material, while the lower crust samples were fuel rods surrounded by previously molten material with a different composition than the upper crust. The solid plugs were 6.4 cm in diameter (the size of the core bore) and ranged from 5 to 11.5 cm in length.

The previously molten region between the crusts appeared to be relatively homogeneous and was easily friable. However, the amount of material present between the crust layers was less than the amount expected based on the video inspections of the core holes. The presumed cause of the less than expected quantities of material was that the friable material fragmented and about 80% was flushed out during the core boring operation by the cooling water. The remaining 20% was characterized as "rocks" (large particles of debris) of various sizes. There were some 100 rocks larger than 2.5 cm in diameter present in the core bores.

The fuel rod stubs located in the lower portion of the core bores ranged from 76 cm to 122 cm in length. Shorter stubs were located near the center of the core and longer ones near the periphery. Initial examinations of these rods suggest that the bottom portion of the rods probably remained covered with water during the accident.

The initial examinations performed on the core bore samples included weighing all samples and performing immersion density and open porosity measurements on the eight large plugs of crust material, and 35 of the 100 rock samples. The densities for the 44 samples ranged from 5.44 g/cm^3 to 9.74 g/cm^3 and the open porosity varied from 5.5 to 19%. The densities measured are from 6.5% to 48% less than the density of intact fuel material (10.4 g/cm^3) which suggests that little intact fuel material material is present in the core bore samples. The lower densities are a result of several factors including porosity and the presence of less dense oxidized zirconium and structural materials. The samples with the lowest density were mostly metallic and quite porous, while the samples with the highest density were generally agglomerates of fractured fuel pellets surrounded by previously molten materials.

GAMMA SPECTROSCOPY EXAMINATION OF THE INTACT CORE BORES

This section presents the results of the high resolution gamma ray spectroscopy measurements that were performed on the nine core bores. Initially each core bore was scanned over the entire length to determine the gross gamma ray intensity as a function of position along the axial centerline of each bore. Following the gross gamma analyses, isotopic measurements were performed at intervals of 2.5 cm over the length of each core bore and at additional locations of high activity as indicated by the gross gamma radiation surveys.

Examination of the results of the gross and isotopic surveys of the core bores allow several observations to be made concerning fission product behavior in the lower reactor core:

- The gamma spectroscopy data suggest that the upper and lower crust regions contain significant concentrations (10^1 -10^2 greater than expected) of ^{60}Co, ^{106}Ru, and ^{125}Sb. These radionuclides would be expected to remain as metallic materials and the metallurgical data indicate that they may have segregated and been retained with other metallic components of the core.

- The prior molten material between the crust layers appears to have very low concentrations of the more volatile radionuclides such as ^{137}Cs but has retained significant amounts of the refractory radionuclides (e.g., ^{144}Ce and ^{154}Eu).

- The intact fuel rod sections in the lower core appear to have retained their entire inventories of fission products including the high volatiles (e.g., ^{137}Cs).

METALLURGICAL EXAMINATION RESULTS

Following the initial nondestructive examinations performed on the core bore samples, samples were selected for metallurgical examinations based on appearance, density, and radionuclide content. Samples were obtained from the crust material, the previously molten material from between the crusts, the intact fuel rods, and intact structural components such as control rods, guide tubes, and burnable poison rods. The largest plug samples were sectioned and sampled both transversely and longitudinally to evaluate radial and axial differences in structure and composition. The rock samples were sectioned into either halves or thirds, depending on the size of the particles, to provide samples of the interiors for both metallurgical and radiochemical examinations. For each sample mounted for optical examination, adjacent samples were obtained for radiochemical analyses to allow comparison of the metallurgical results with the corresponding radiochemical composition of the material. The examination results discussed in this paper are from representative samples of the upper, lower, and peripheral crusts, the mixed ceramic and metallic material present in the region between the crusts, and the fuel rod stubs.

Lower Crust

Samples of the lower crust material were obtained at several core bore locations. Figure 3 shows a cross section and the autoradiograph of a representative plug of the lower crust taken from near the center of the core (core location K9). The measured density of this crust sample was 7.2 g/cm^3. The cross section shows the remains of two fuel stack columns surrounded by previously molten material. Molten material apparently flowed down the coolant channels, dissolved the zircaloy cladding, and flowed into the pellet/pellet interfaces and cracks in the pellets.

Several areas of this cross section were examined using optical metallography and back scattered electron (BSE) image analysis. Figure 4 shows an enlarged view of the previously molten material found in the coolant

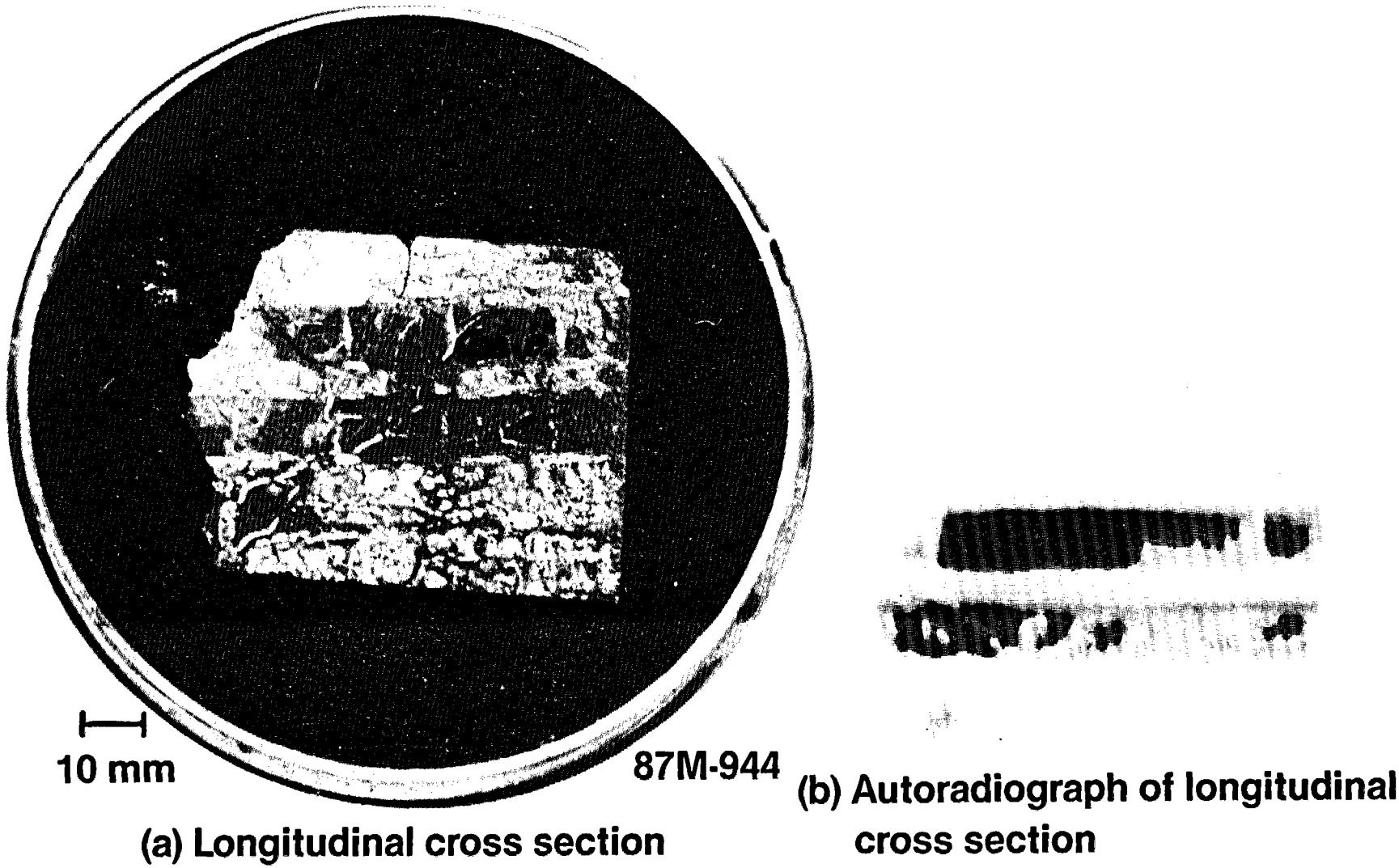

Figure 3. Core location K9--lower crust.

Figure 4. Enlarged view of molten material in the coolant channel.

channels. This material was composed of a mixture of metallic structural and control rod components with relatively small (100 - 200 micron) UO_2 inclusions. Two metallic phases were present as determined from the BSE analysis. The principal phase consisted of zirconium, iron, nickel, and chromium and the secondary phase contained an alloy of silver and indium.

Figure 5 shows an enlarged view of the area at a pellet/pellet interface which is typical of the interfaces in this sample. Figure 6 shows the BSE images for this pellet/pellet interface and the BSE dot maps for U, Zr, and Fe. This figure typifies the method used to identify the composition of the various phases present in a sample. The BSE image represents a composite average of the atomic number of the elements in a particular phase where the degree of brightness is proportional to the atomic number of the element (e.g., the high atomic number uranium is brighter than the lower atomic number iron) and the individual dot maps represent specific elements where the element of interest is brighter than the other elements present in the sample. The uranium and zirconium dot maps in Figure 6 show the presence of a UO_2 pellet above a region in the pellet/pellet interface which contains mostly zirconium with small amounts of uranium.

Other metallic phases are also present in the channel as indicated by the Fe dot map which indicates the interaction of zircaloy with structural and control materials. Several metallic phases were observed which were composed of the following groups of elements (Zr, Sn, Ni, Fe), (Zr, Fe, Cr, Ni, U), (Zr, Ni, In, U), and (Ag, In). Cadmium, a component of the Ag-In-Cd control rods, was found with the Ag and In phases; however, it was present in relatively small amounts. This is probably due to the relatively high volatility of this element (B.p. - 940 K). Also, when Zr was alloyed with In, Fe and Cr were not present. The mechanism resulting in this behavior is not currently understood.

The metallographic examination of the lower vessel plug samples suggest that an interaction occurred between the fuel rods and the structural components (i.e., Fe, Cr, etc.) which resulted in the dissolution of the zircaloy cladding and fuel by the molten structural materials. This interaction would result in a lowering of the melting temperature of the material. Based upon the eutectic temperatures of the binary phases of zirconium with Fe, Ni, or Cr, a minimum possible peak temperature is estimated to be about 1400 K and because there was not an interaction with the unmelted UO_2 fragments, a maximum peak temperature of 2200 K is suggested.

In addition to the metallographic examination of the lower crust autoradiography was performed to evaluate the gross distribution of fission products in the crust. This examination indicated that the fission products in the lower crust were retained within the fuel material and that little activity was present in the metallic debris in the coolant channels.

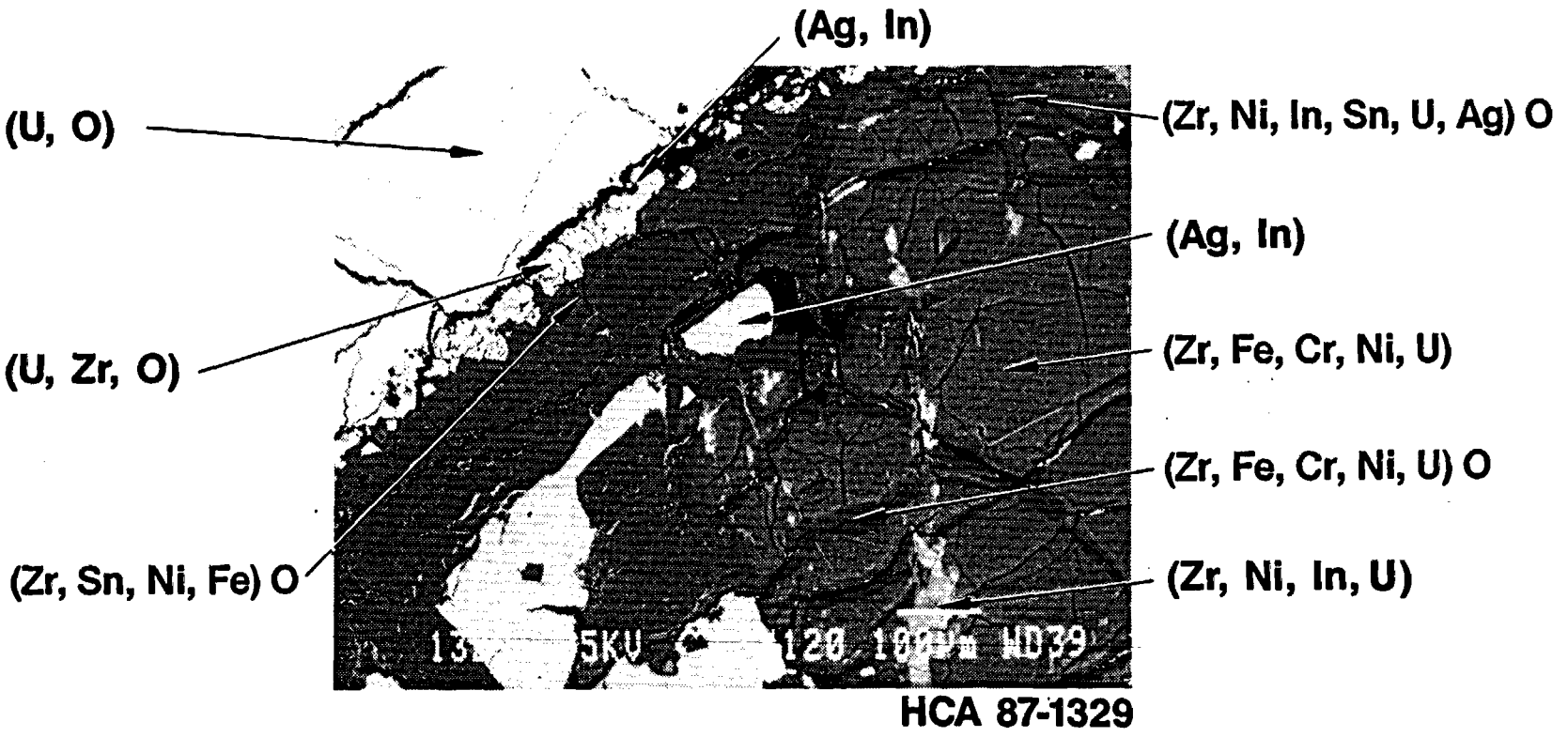

Figure 5. Enlarged view of the pellet/pellet interface.

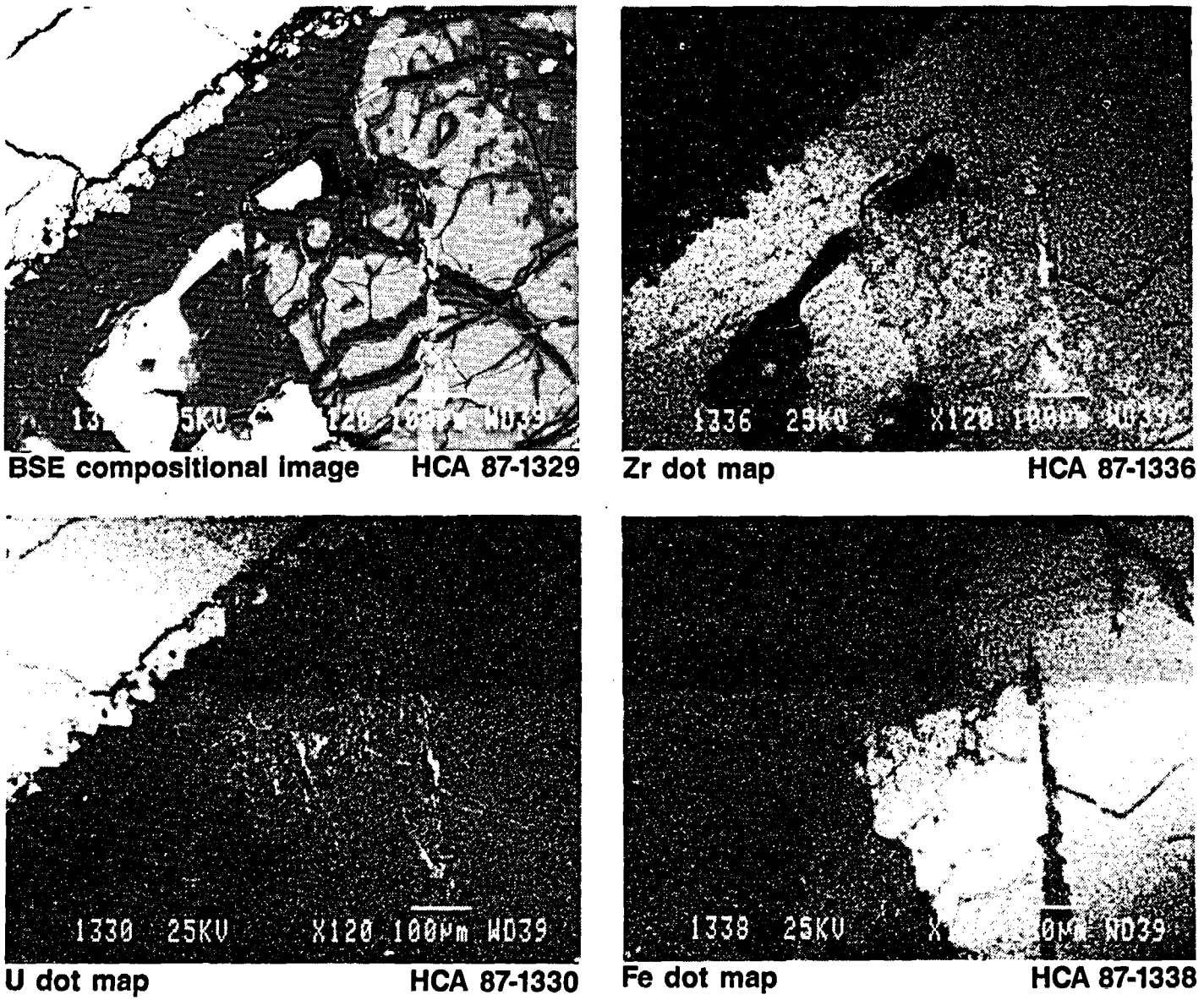

Figure 6. Pellet interface--BSE image and dot maps.

Upper Crust Plug

Figure 7 shows a representative cross section of upper crust material obtained from core bore K9 about 1 meter above the sample discussed in the previous section (Figure 3). The bulk density of this plug section was 7.9 gm/cm^3. Two general types of phases were observed in the upper crust, a ceramic phase containing mostly fuel material components and a metallic phase containing mostly structural components. The composition of the ceramic phase indicated that the interaction between fuel rods and structural/control rod materials was substantially greater than that observed in the lower crust samples. No intact fuel material was present and most structural materials were present as oxides except those which do not oxidize easily (e.g., Ni, Ag and In). The BSE images indicate that the ceramic phase was a mixture of oxides of uranium and zirconium with an average composition of about 56% U and 21% Zr with small amounts (about 1%) of iron, chromium, and nickel in solid solution. Based upon this composition for the ceramic mixture, the peak temperature of this layer was estimated to be about 2800 K.

The metallic phase found in the upper crust was principally composed of iron and nickel; however, as was indicated for the lower crust, a second metallic phase was observed which was principally composed of metallic silver and indium. Unlike the lower crust, however, the upper crust did not contain measurable amounts of Cd, which suggests that the greater degree of materials interaction in this crust allowed most of the relatively volatile Cd to be released.

In contrast to the fission product behavior observed in the lower crust, the autoradiograph of the sample cross section from the upper crust indicated higher concentrations of fission products in the metallic phases rather than in the ceramic phases. The probable identities of the fission products in the metallic crust (i.e., Sb-125 and Ru-106) were indicated by the gamma spectroscopy measurements discussed previously. These radionuclides are expected to be retained as metallic materials in the debris rather than as oxides because of high free energy requirements for oxidation. Other examinations indicate that these fission products are associated with metallic components of the TMI-2 debris[4]. The ceramic phase of the debris is probably depleted in fission products (e.g., Cs-137) which have relatively high volatilities and were released from the ceramic phases during the high temperature portion of the accident.

Peripheral Crust

The peripheral crust is that region of the upper crust that is near the mid-radius of the core. Densities in this part of the crust range from 8-10 g/cm^3 and are generally higher than those observed near the center of the core. A representative cross section from the peripheral crust (core location G8) is shown in Figure 8. Examinations of this cross section and others from the peripheral crust indicate that the materials behavior in this part of the core is different than that observed in the upper and lower crust regions. The presence of substantial amounts of metallic structural components (i.e., Fe, Ni, Ag, and In) is indicated. In Figure 8, the light

Figure 7. Core location K9--upper crust.

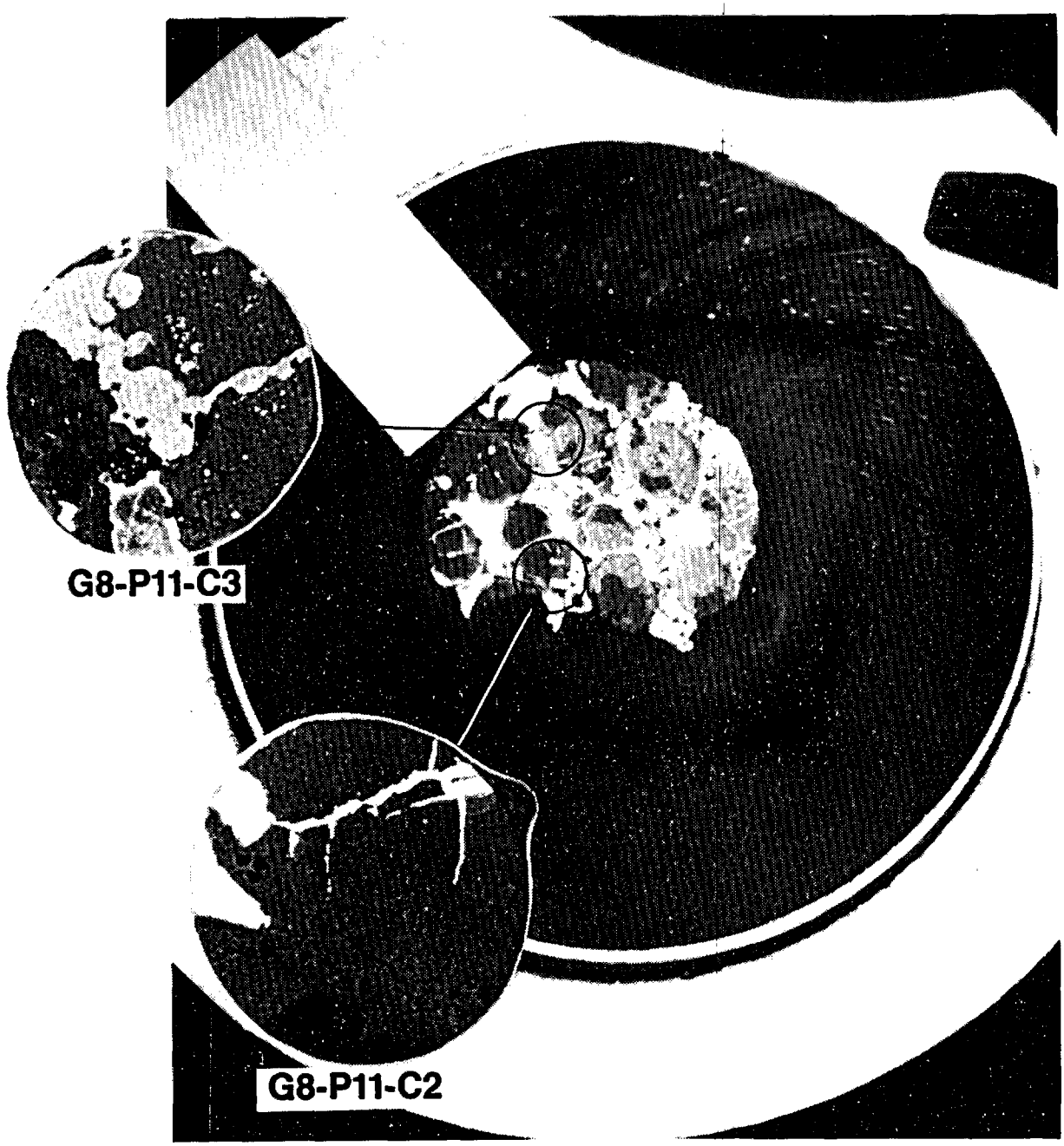

Figure 8. Core location G8--peripheral crust.

areas shown in the enlarged section of G8-P11-C3 are a silver-indium alloy which appears to have flowed into cracks in the ceramic material. Adjacent to this inclusion is a secondary phase containing iron and nickel with a small amount of chromium. The presence of unmelted fuel in the surrounding material suggests that unmelted fuel from the upper debris bed may have slumped into the molten metallics.

A second cross section from the peripheral crust at core location G12 (Figure 9) shows intact fuel pellet remnants encased in a ceramic matrix of mixed oxides of uranium and zirconium. This figure shows an apparent interaction at the fuel pellet/ceramic interface which has resulted in the formation of large (1-4 mm) voids throughout the fuel pellets. This behavior may have been caused by the collapse of relatively intact fuel pellets from the upper debris bed into molten material which then heated the relatively intact material to high temperatures. The actual cause of the porosity is not known.

Autoradiographs of the peripheral plug cross sections were taken. These data indicate the presence of significant accumulations of activity in the metallic phases, similar to the behavior observed in the upper crust samples.

Core Interior Particles

Metallographic examinations were performed on 26 "rock-like" particles from the previously molten material region between the crust layers. The rock samples examined were greater than 25 mm in diameter and were selected based on density, and surface appearance. Although individual particles were relatively homogeneous, the metallographic examinations indicated a diversity of structure and composition between particles. The bulk of the samples examined were determined to be mixtures of both metallic and ceramic phases, however, examples of entirely ceramic and metallic particles were also present. Examples of each of the material types are discussed in this section.

A BSE image of an entirely ceramic particle (K9-P3-F) is shown in Figure 10. Examination of this particle indicated that this was a relatively homogeneous ceramic rock with a number of low atomic number inclusions present. An area at an interface between the light and dark areas was examined using dot maps to evaluate the composition of these phases. The light phases in the examination area were determined to be mixtures of uranium and zirconium and the dark (lower atomic number) regions were determined to be mixtures of iron, chromium, aluminum, and nickel oxides. The presence of nickel oxide in the sample suggests that this sample was subjected to very oxidizing conditions as nickel has a very high oxidation potential and would not be expected to be oxidized by steam oxidation only. Particles of this type resemble rock-like particles of previously molten material obtained from the lower reactor vessel head which contained oxides of uranium and zirconium in the matrix and iron and chromium oxide eutectic mixtures in the grain boundaries[4].

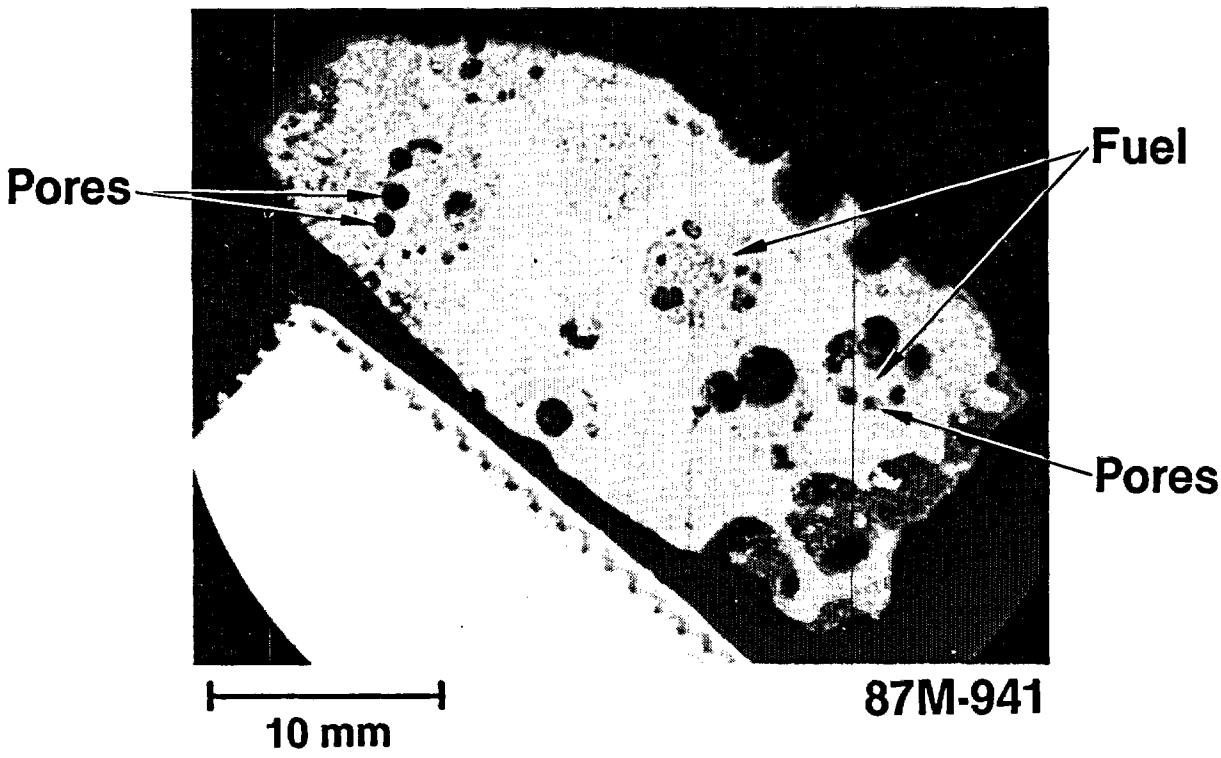

Figure 9. Voids produced in fuel pellets in the peripheral crust.

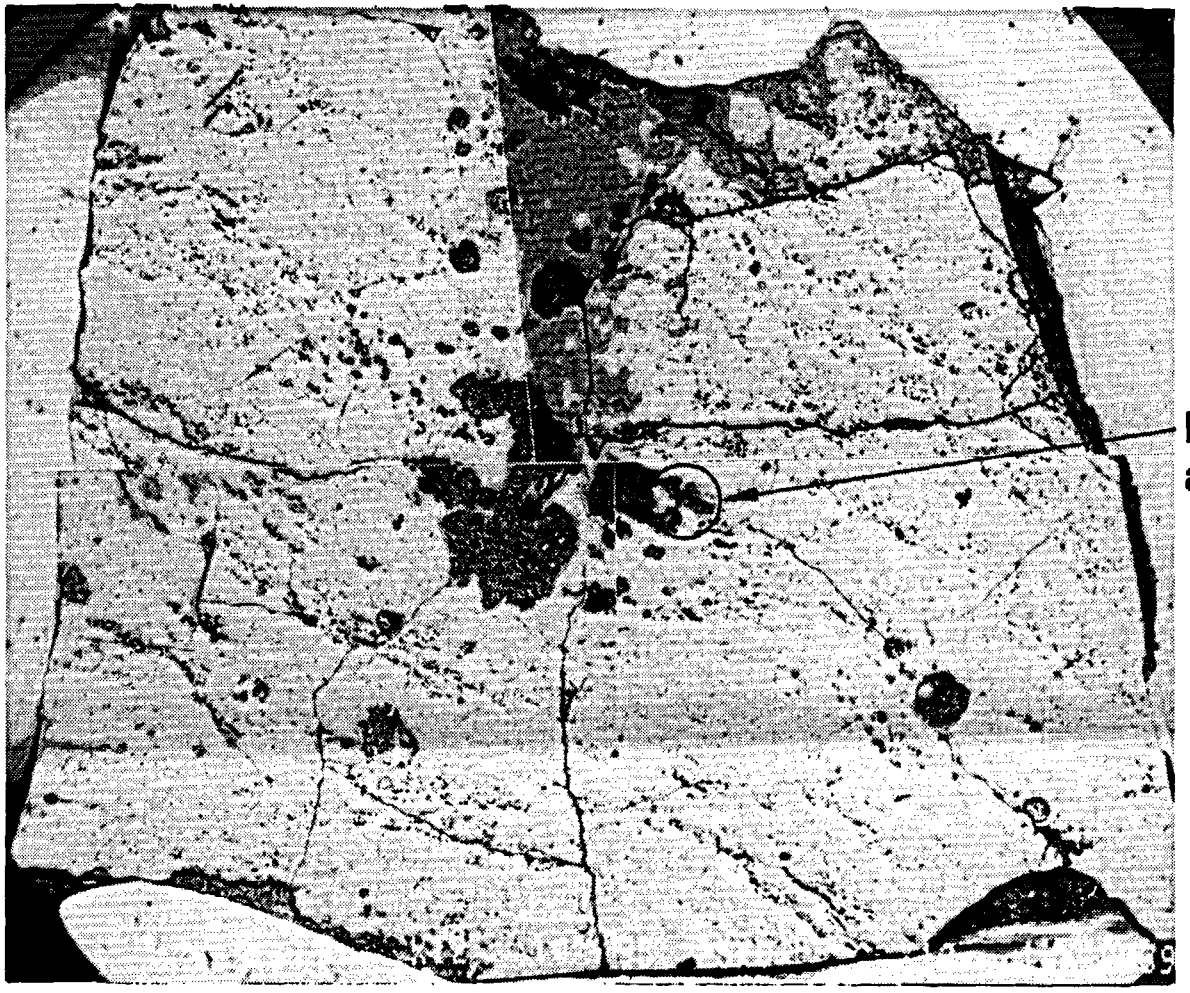

Figure 10. Core location K9--ceramic particle (BSE image).

Figure 11 shows an entirely metallic sample which was obtained from fuel assembly location 09 near the periphery of the core. The metallic matrix of this sample consisted of a nearly dendritic structure of 59% iron, 25% nickel, and 14% chromium with circular inclusions containing silver, indium, and tin (72% Ag, 15% In, and 9% tin). Although some of these Ag-In-Sn inclusions contained voids, many contained a spherical particle of chromium oxide (Cr_2O_3).

A cross section of a particle (core location G12) which contained a ceramic matrix with extensive metallic inclusions is shown in Figure 12. One of these inclusions was examined by SEM to evaluate elemental composition. The BSE image and several associated dot maps are shown in Figure 13. These data indicate that a large degree of segregation of individual elements took place in this sample. The ceramic matrix of the sample is a mixture of the oxides of uranium and zirconium and, at the periphery of the void containing the inclusion, is a layer of iron oxide which contains some oxidized nickel. In the metallic inclusion, there is substantial segregation of the elements. At the bottom of the inclusion relatively pure silver is found with little contamination from other metallic elements (i.e., indium and cadmium). Above this layer, near the particle midpoint, is a nickel-tin layer followed by a zone containing nickel with nickel-tin inclusions. Also in the nickel region, concentrations of the fission product ruthenium were found as a metallic. These data suggest that this fission product, which has a high free energy requirement for oxidation, is released from the fuel and is retained by metallic structures in the core. The materials behavior responsible for the observed structures has not been well defined and additional information will be required to understand this behavior.

The most common fission product measurable in the metallic inclusions of this rock sample was ruthenium; however, technetium, a fission product not found in nature was also measurable. Also, palladium and tellurium, other probable fission products, were measured in association with metallic constituents (i.e., Ag, In, and Fe). These data suggest that the metallic constituents of the core retain fission products with varying chemical characteristics and volatilities that have been released from the fuel material.

A beta/gamma autoradiograph of several different particles is shown in Figure 14. Because the radiograph was performed on all samples with only one exposure time, the intensity of the radiographs may be used as an indicator of the relative activity among the particles. The ceramic particle (G8-P6-B) has the lowest activity which is about the same as the ceramic phase of the mixed ceramic/metallic particle (G8-P10-A). The metallic particle and the fuel remnant surrounded with metallics also have about the same activity as the metallic phase in G8-P10-A. These data again indicate significant release or depletion of the activity in the ceramic phases and suggest similar retentions for all ceramic or metallic components.

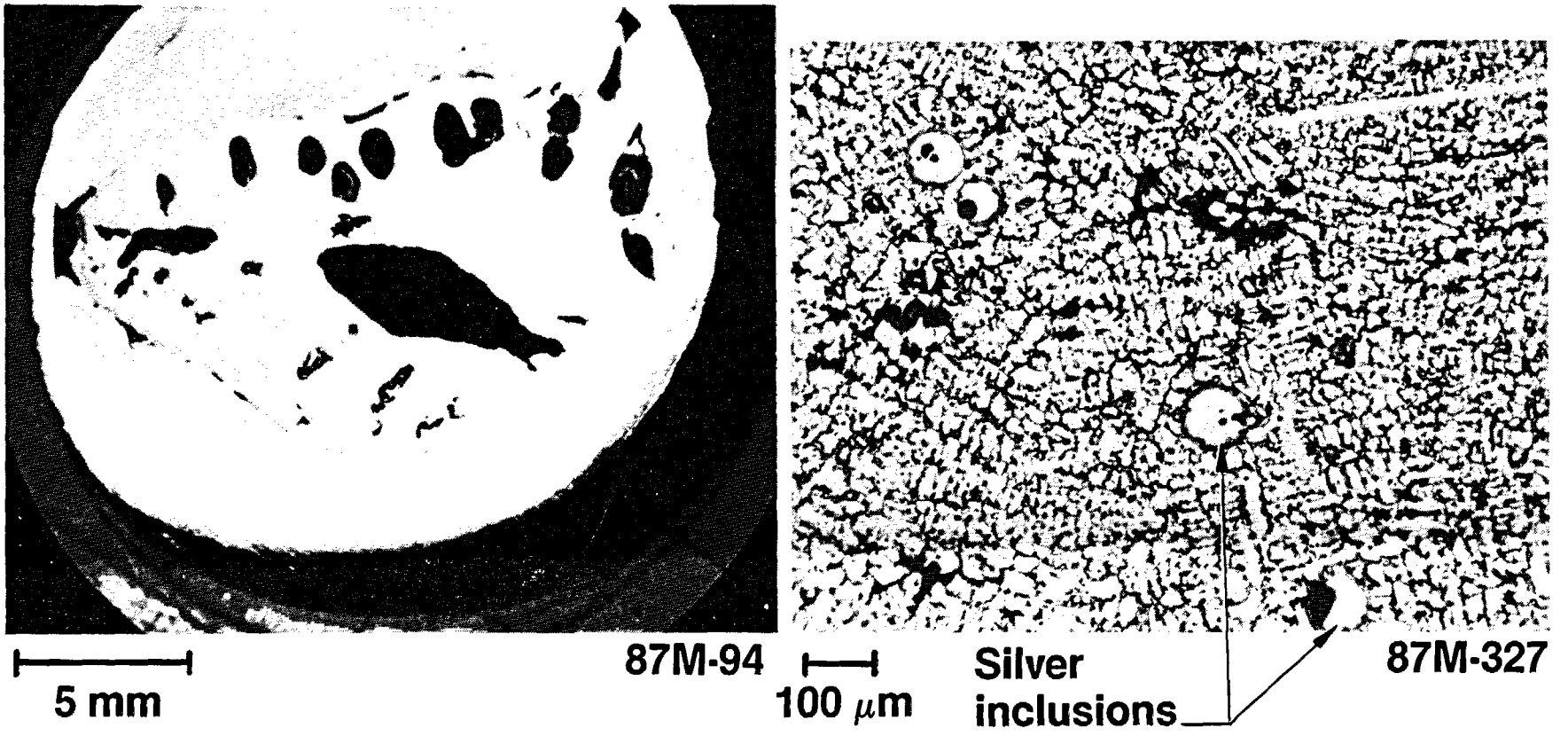

Figure 11. Core location 09--metallic particle.

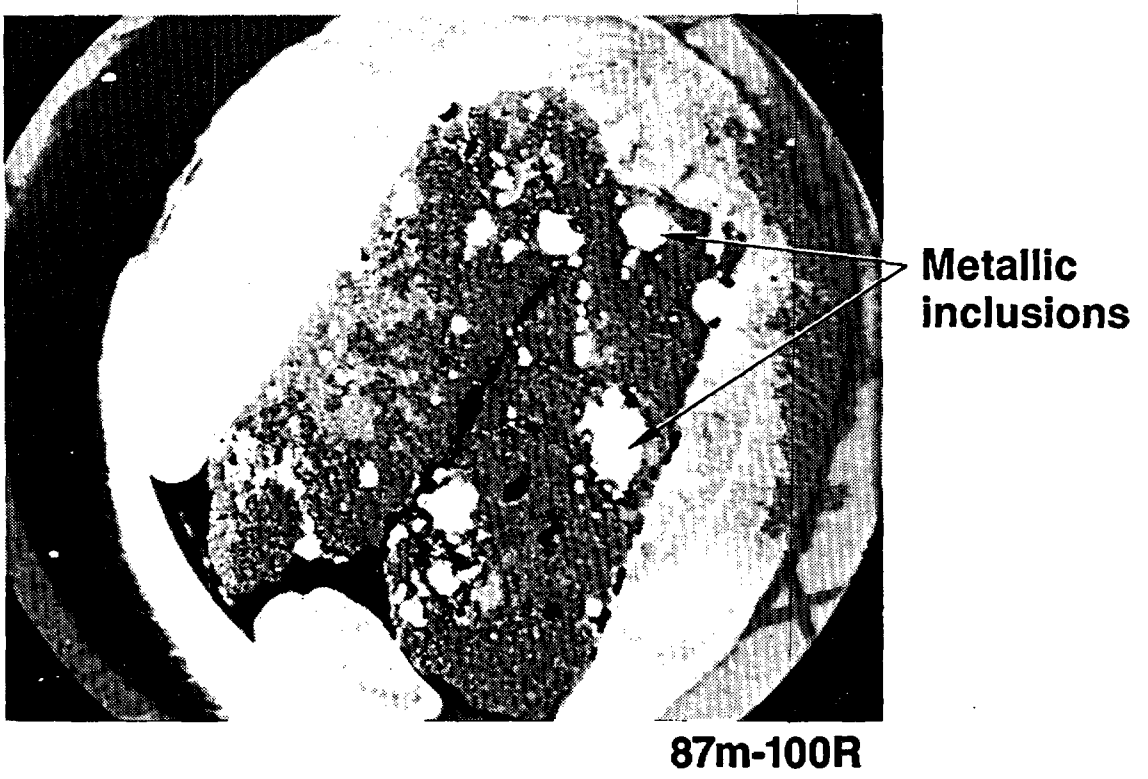

Figure 12. Ceramic particle with metallic inclusions (core location G12).

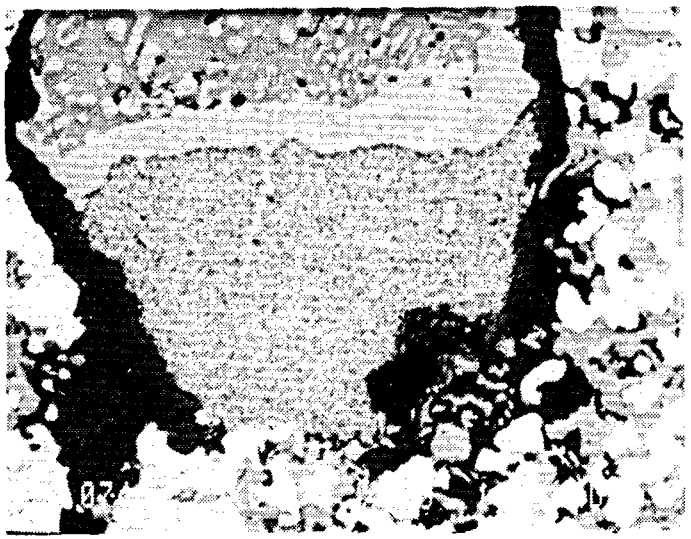

BSE compositional image HCA 87-742

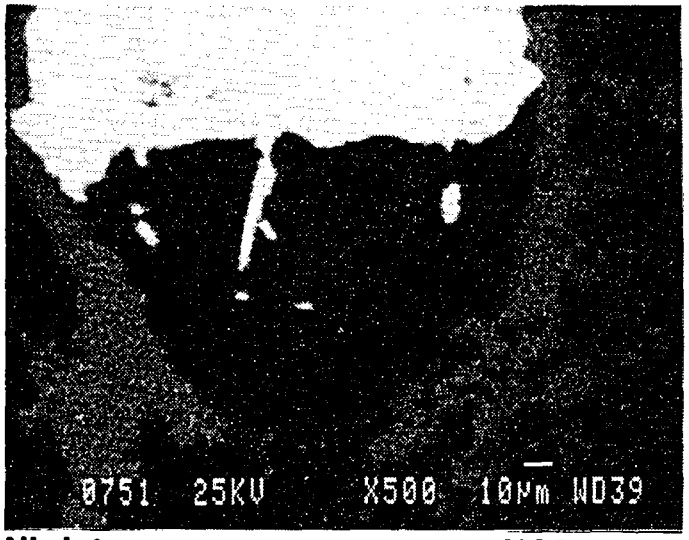

Ni dot map HCA 87-751

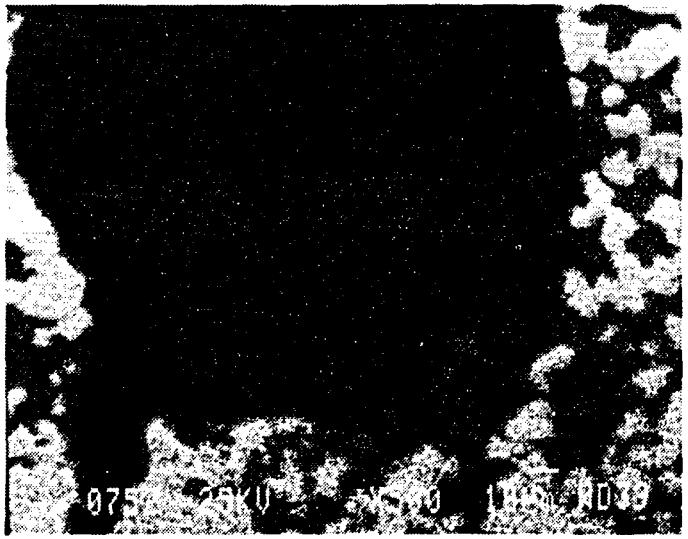

U dot map HCA 87-752

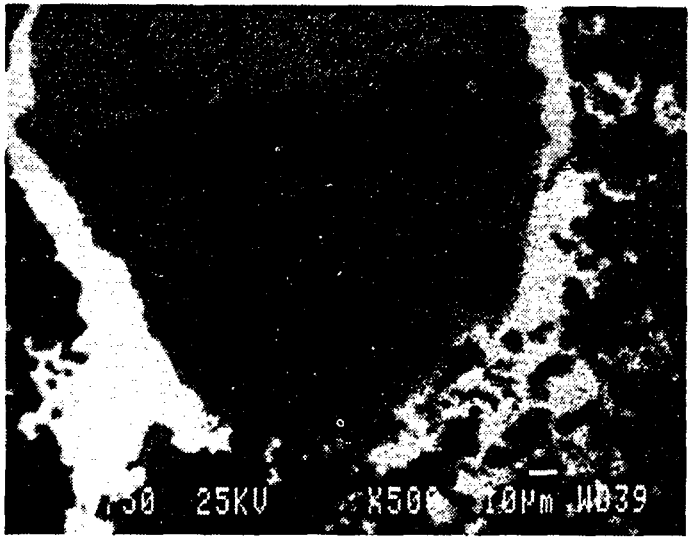

Fe dot map HCA 87-750

Figure 13. Enlarged metallic inclusion from core location G12 (BSE image and dot maps).

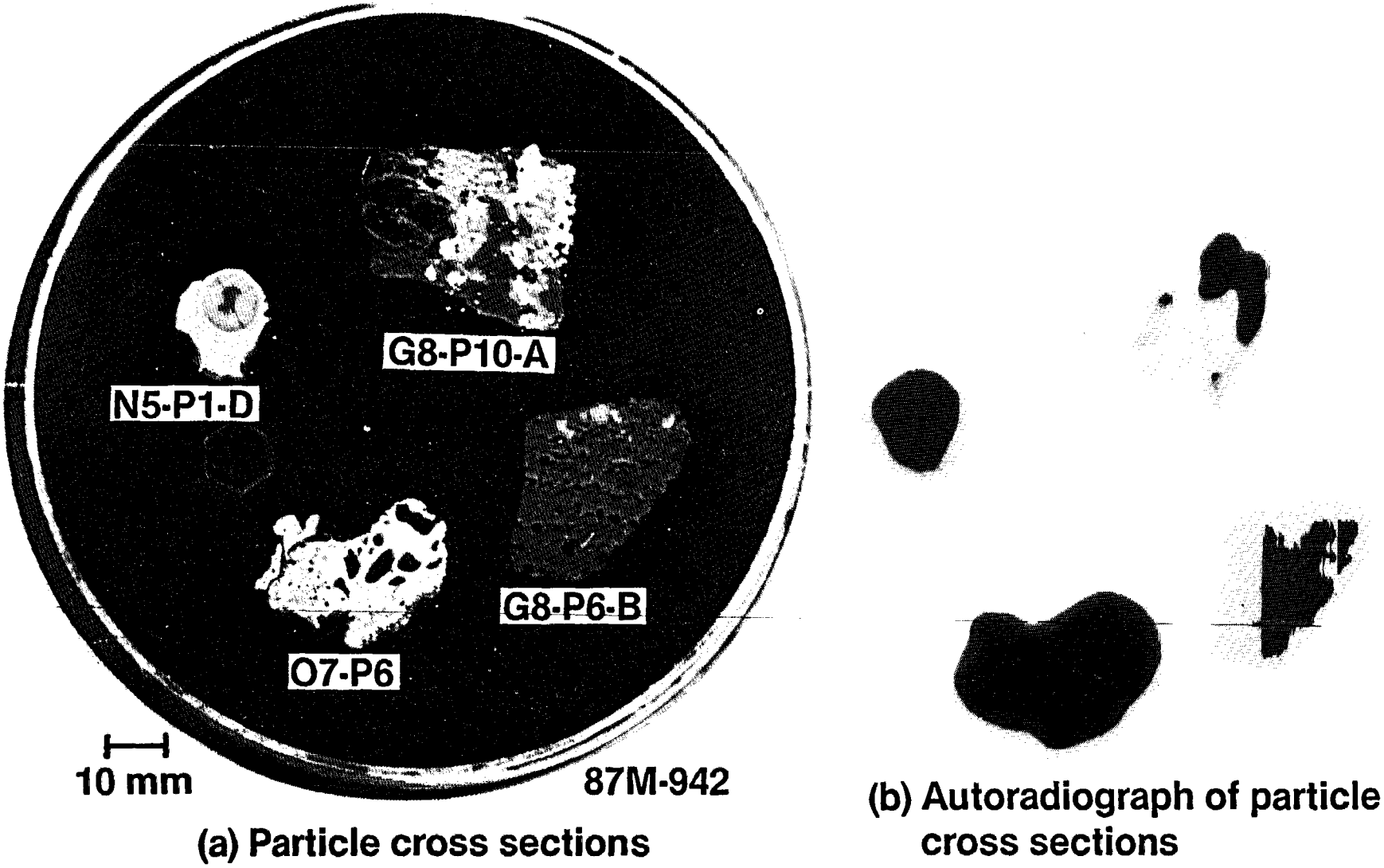

Figure 14. Core locations N5, G8, and O7--particle cross sections and autoradiographs.

Fuel rods and guide tubes

Fuel rods, and guide tubes from the lower portion of the reactor core were examined to evaluate the effects of the accident on the intact rods or tubes. Visual examination of the rods indicated that the rods were generally intact, however, the metallurgical examination indicated that hydriding of the fuel rod and guide tubes had occurred. The hydrides were orientated in the radial direction, which is typical for the cold-work texture of the cladding. Examinations performed on fuel rods at the INEL and at Argonne National Laboratory[5] indicate that the cladding temperature reached temperatures up to 1100 K.

Although no previously molten debris was present between the intact fuel and control rods in the core bores, previously molten material was found in an instrument tube in Assembly G8. The molten material which had apparently flowed down into the zircaloy tube and interacted with the interior surface of the tube was composed mostly of zirconium with some iron and nickel. It also contained relatively small quantities of silver, indium and cadmium from the control rods.

SUMMARY

A summary of the observations and conclusions that have been made from the core bore examinations are listed below. The core bore examination program is not complete and additional information will be provided in the final examination report.

- The lower crust was formed by freezing of relocated molten cladding, structural, and control materials into the fuel assembly coolant channels. Peak temperature of this crust was probably between 1400 K and 2200 K.

- The upper crust is a mixture of previously molten ceramics, metallics, and solid fuel pieces with an estimated maximum temperature of 2800 K.

- The metallic structures in the upper crust are composed primarily of structural (Fe, Cr, and Ni) and control materials (Ag, In, and Cd).

- A range of densities were found in the upper, lower and peripheral crust samples with the higher densities found in the peripheral crust probably due the lower porosity and greater proportion of higher density metallics (e.g., Ag).

- Fission product ruthenium and antimony were retained in the metallic phases of the upper crust and core rocks (mixed ceramic and metallic particles).

- o In the previously molten material region, cesium is at substantially lower concentrations than would be expected for intact fuel material.

- o The radionuclide inventory of the intact fuel rods, including the more volatile radionuclides (e.g., Cs-137) appears to be intact.

- o Cadmium was not detected in the upper crust of the central core region; however, small quantities of Cd were detected in the lower crust.

- o A zircaloy instrument tube at the G8 core location provided a pathway where prior molten fuel flowed down into the tube and interacted with the zircaloy of the tube.

- o Particles of prior molten fuel from the central core region had a wide variety of compositions. Most were a mixture of ceramic and metallic components; however, some were entirely metallic or ceramic.

REFERENCES

1. M. L. Russell et al., TMI-2 Accident Evaluation Program Sample Acquisition and Examination Plan for FY 1987 and Beyond, EGG-TMI-7521,February 1987.

2. D. W. Akers et. al., TMI-2 Core Debris Grab Samples--Examination and Analysis, GEND-075, September 1986.

3. E. L. Tolman et. al., TMI-2 Core Bore Acquisition Summary Report, EGG-TMI-7385, Rev. 1, February 1987.

4. C. S. Olsen et. al., Examination of Debris from the Lower Reactor Head of the TMI-2 Reactor (Draft), EGG-TMI-7573, April 1987.

5. L. A. Neimark et. al., Examination of TMI-2 Core Bore Samples, 15th Water Reactor Safety Research Meeting, October 26-30, 1987 (to be published).